СООБЩЕНИЯ
ОБЪЕДИНЕННОГО
ИНСТИТУТА
ЯДЕРНЫХ
ИССЛЕДОВАНИЙ

Дубна

E10-99-151

V.Zagrebaev, A.Kozhin

NUCLEAR REACTIONS VIDEO

(Knowledge Base on Low Energy Nuclear Physics)

1999

1 "Nuclear knowledge base" – What is it?

1.1 Motivation

There are two problems encountered by every physicist (both an experimentalist and theorist) in his everyday work on processing experimental data or preparing new experiments: (1) search for available experimental data on nuclear properties and nuclear reactions and treatment of these data, (2) analysis of the processes under study within reliable theoretical models of nuclear dynamics. The first problem can be solved at best as follows. A user looks for appropriate nuclear database, finds required nucleus, and writes out the value of parameter he needs. There are several well-known and permanently renewed nuclear databases (see [1-8] and other references/links therein). However, most of these databases are formed like ordinary text tables (easily accessible and visible via Internet) or like downloaded files. So, if you want to obtain some systematics over a group of nuclei (for example, separation energy of two neutrons from the isotopes of a given element) and view a plot, you have to write out several tens of numbers, make some calculations (even rather simple), obtain a table, and use some graphic package to draw a plot.

More complicated problems appear when we solve the second task – analysis of experimental data within theoretical models of nuclear dynamics. There are very effective and reliable theoretical approaches to description of low energy nuclear reactions and nuclear structure: optical model of elastic scattering, distorted wave Born approximation, channel coupling approach, statistical model of nuclear decays and fission, shell model, and many others. However, the corresponding computer codes are written, as a rule, in Fortran. They have a long lists of instructions on preparation of input data and make the calculations "blindly" without a possibility of watching the dynamics of the process under study to understand it quite clear. The final results are presented in the tabular form demanding their subsequent processing with some graphical tools. Finally, these codes are very difficult in management and are commonly used either by the authors or by trained specialists occasionally specially invited. Note that even for theorists, who understand the models themselves well, it is not so easy to use somebody else's codes for overall analysis of the investigated process. This situation leads to artificial specialization of physicists who are experienced only in one model, and also to a loss of unity in performing and treating the physical experiments, all this requiring additional time and expenses. Creation of the effective "low energy nuclear knowledge base" could help us solve these problems.

1.2 Main ideas and principal scheme

These well-established and commonly used models of low energy nuclear dynamics (such as the optical model, DWBA for transfer and breakup reactions, channel coupling method, transport equations of the deep inelastic process and fusion, statistical model of decay of hot nuclei, few body molecular dynamics, shell model, liquid drop model, and many others) have to be arranged in the way so that to be accessible and easily used by any inexperienced (in sense of programming) scientist working in the field of low energy nuclear physics. The total set of the intersected algorithms of nuclear dynamics must lean on the experimental nuclear database and be controlled by a common multi-paged interface altogether forming what is usually called "knowledge base". A principal scheme of this nuclear "knowledge base" is shown in Fig.1.

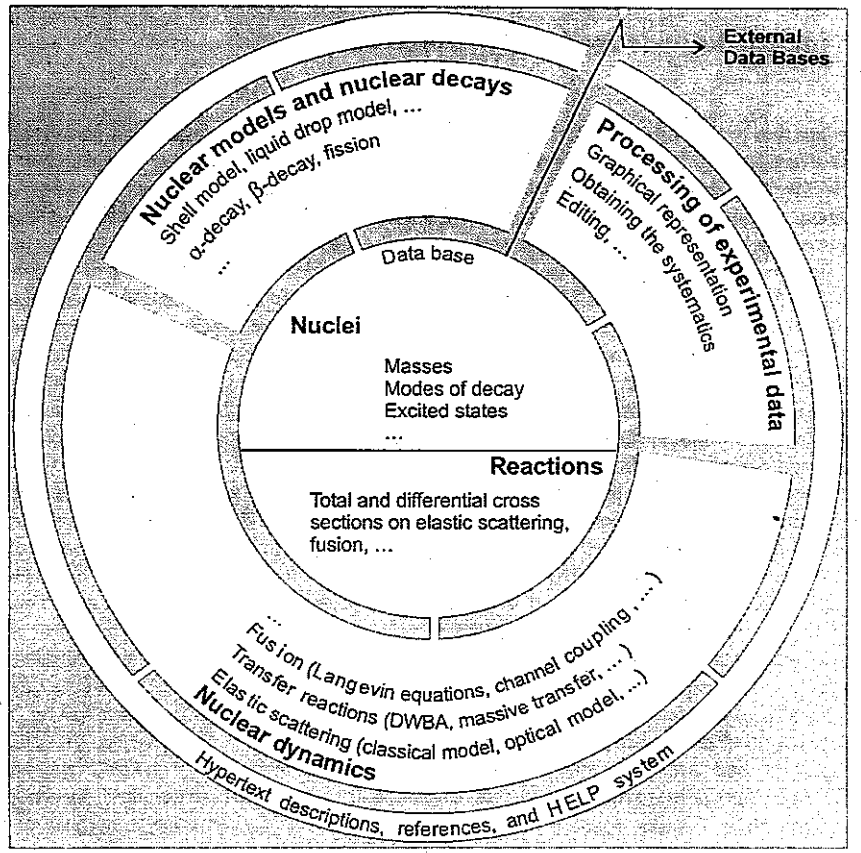

Fig. 1 Principal scheme of the low energy nuclear knowledge base NRV

Creation of the NRV system is based on realization of the following principal points.

(1) Net and program compatibility with existing nuclear databases [1-2]. It provides us with renewed and permanently extended experimental information on basic nuclear properties such as nuclear masses, modes of decay, half-lives, excited states, and so on.
(2) Maximal simplicity in handling. This is assured by the widely branched menu, visual graphic representation of all information, hypertext descriptions, references, and HELP system.
(3) Maximal visualization of all input data, dynamics of the investigated process, and final results by means of real images, plots, tables, formulas, and 3-dimensional animation.
(4) All software are operated under Windows 95/NT. This solves the problem of compatibility of the NRV system with any peripheral devices and with such commonly used software as Corel Draw, Origin, Microsoft Word, and other Windows applications.
(5) Accessibility of the "knowledge base" via standard local and global computer nets.

1.3 Operation system, data base format, and coding

A choice of operation system is very important for such a software like the NRV. Unfortunately there is no a unified operation system used by all physicists. Some people work with UNIX, others prefer Windows. We chose the latter because, as it seems to us, there is more advanced and faster developing software created just under Windows. This operation system is supported now not only by IBM but also by Macintosh personal computers.

Using C++ as a main coding language (Borland C++ compiler under Windows) we obtain a powerful tool for building our main classes of graphical support (including a 3-dimentional one), numerous interface dialogs, handling the database, and all the algorithms of nuclear dynamics. The BDE_IDAPI SDK and IDAPI functions are used in the work with our database. The DBF representation of the experimental data on nuclear properties is sufficiently convenient to work with them and can be easily changed if some other format would be found to be more appropriate for a net version of the NRV. At present all experimental data are divided in several DBF-tables (masses, modes of decay, energy levels, and so on) which can be downloaded separately in case of need. As already mentioned, these data can be renewed and edited directly using the basic external databases or some other sources of information.

All the algorithms of nuclear dynamics (see below) are written with C++ and formed as real Windows applications, i.e., they can start and operate independently, but they all rest on the same database and have a common starting interface. It means that analyzing, for example, collision of nuclei A and B within different models (elastic scattering, fusion, transfer reaction, ...) one automatically uses the same interaction parameters and other properties of both nuclei in the entrance channel.

1.4 Web expansion and Java applets

We found that the simplest codes of processing nuclear data and some nuclear models can be formed as Java applets and, therefore, be directly accessible through the net with any computer (irrespective of operation system) having a Web-browser supported Java codes, for example, Internet Explorer 4, Netscape Navigator 4, or higher. Advantages of the JavaScript technology in forming and managing nuclear database can be viewed in the Lund Nuclear Data WWW Service as an example [7]. Resemblance of the object oriented languages C++ and Java allows us, in principle, to rewrite most of the simplest Windows applications in the form of full-fledged Java applets. Of course, the available Java compiler (Java Developers Kit) is not so effective and convenient yet as C++ compilers. However, very fast evolution of the Java technology can bring us in nearest future to quite a new situation when the Java language will be used not only for the Web purposes but also for coding very complicated algorithms.

2 Main possibilities and main menu

The main menu of the NRV consists of the following hierarchic items leading to the basic nuclear models and to processing nuclear data. Today some of the models of low energy nuclear dynamics (see below) operate in full capacity, and others are under construction.

Quit		
NUCLEI	**Nuclear Map**	Available Information Systematics Decay chains
NUCLEAR MODELS	**Shell Model** **Liquid Drop Model**	
DECAYS	**Alpha-decay** **Beta-decay** **Fission** **Decay of Hot Nuclei**	
NUCLEAR REACTIONS	**Elastic Scattering**	Classical Model Semiclassical Model Optical Model
	Inelastic Scattering	Coulomb Excitation Direct Process (DWBA) Deep Inelastic Collisions
	Fusion	Classical Model Langevin Equations Empirical Models Channel Coupling Driving Potential
	Transfer Reactions	3-body Classical Model Direct Process (DWBA) Multi-nucleon Transfer
	Breakup Reactions	3-body Classical Model Direct Process (DWBA) Sequential Decay Fragmentation
	Pre-Equilibrium Particles	Classical Models Fermi-jet Model Moving Sources
	Kinematics	2-body Kinematics 3-body Kinematics
Help		

The graphical interface of the main menu - Fig.2 - is a common 'entrance point' to the NRV. In spite of the fact that all the models listed above are prepared as self-dependent Windows applications and can be started separately, one has to pass this 'entrance point' if you want to analyze some process of collision within different approaches keeping the same values of all common parameters of colliding nuclei. It means that the "Input Dialogs" of all the models look very similar to each other and operate with the same set of accumulated variants of different reactions studied by a user of the NRV (see Figs.3 – 5 as examples). Any variant can be changed, deleted, or added to the database only within the main program of the NRV, which, thus, performs the duties of a dispatcher. As can be seen from Figs.3 – 5, there are many common input parameters for different reaction channels of the nucleus-nucleus collision: projectile-target interaction, energy of collision, some properties of colliding nuclei. Thus, it is quite reasonable to have a common DBF table, every line of which completely defines one of the studied collision processes, i.e., all the parameters of the entrance channel and different exit channels.

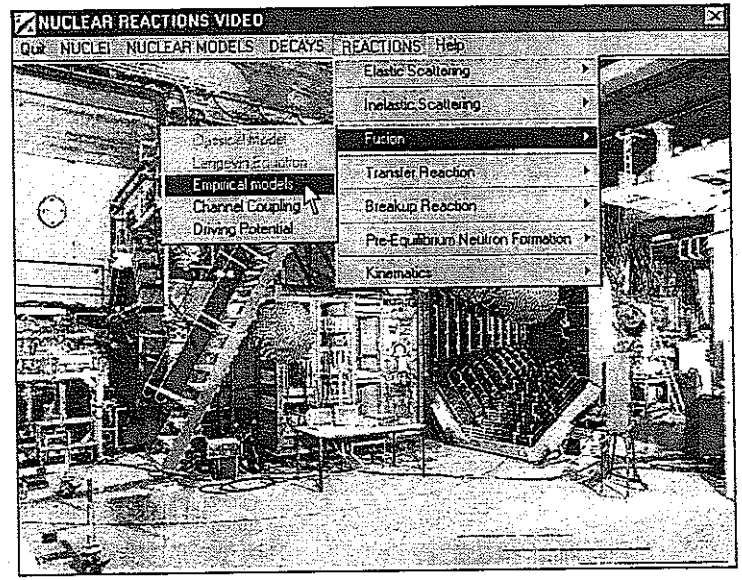

Fig. 2 Animated "entrance window" to the NRV

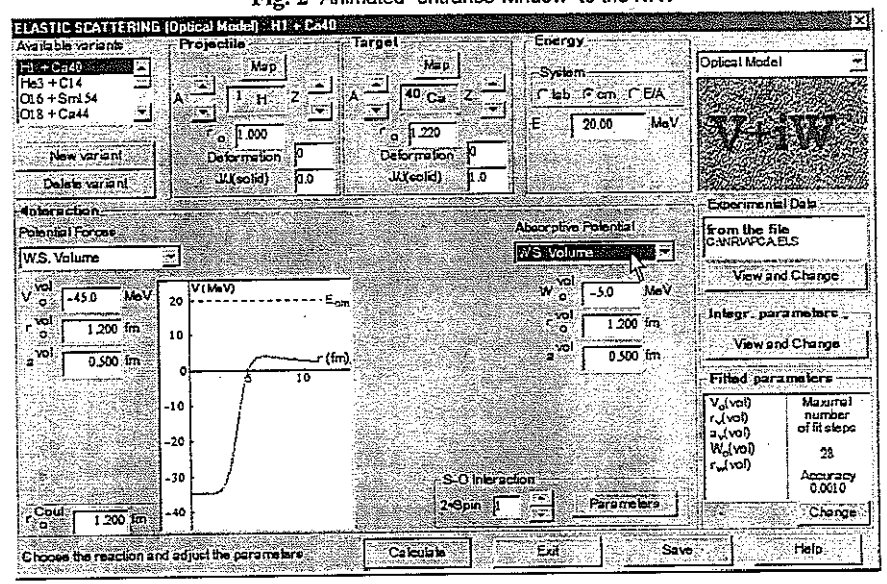

Fig. 3 Main input dialog of the Optical Model code of the elastic scattering

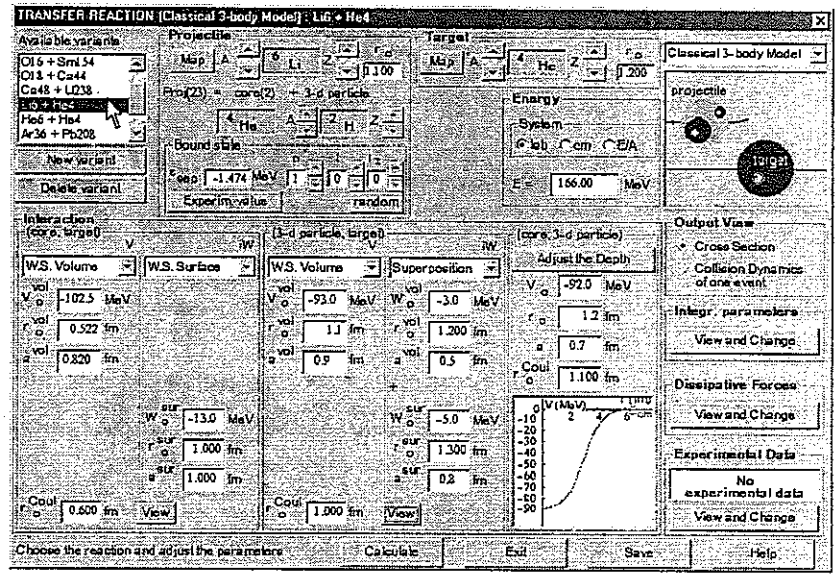

Fig. 4 Main input dialog of the 3-Body Model of the transfer and breakup reactions

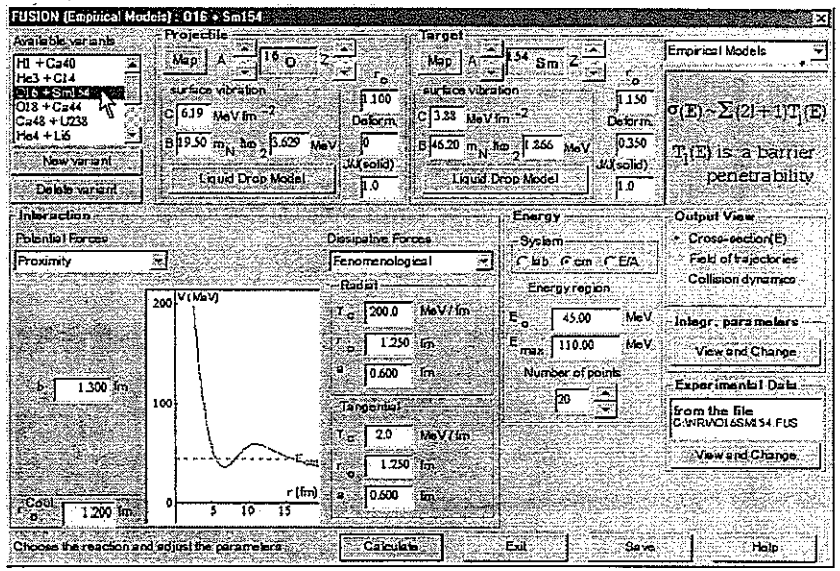

Fig. 5 Main input dialog of the Fusion process of atomic nuclei

3 Nuclear database

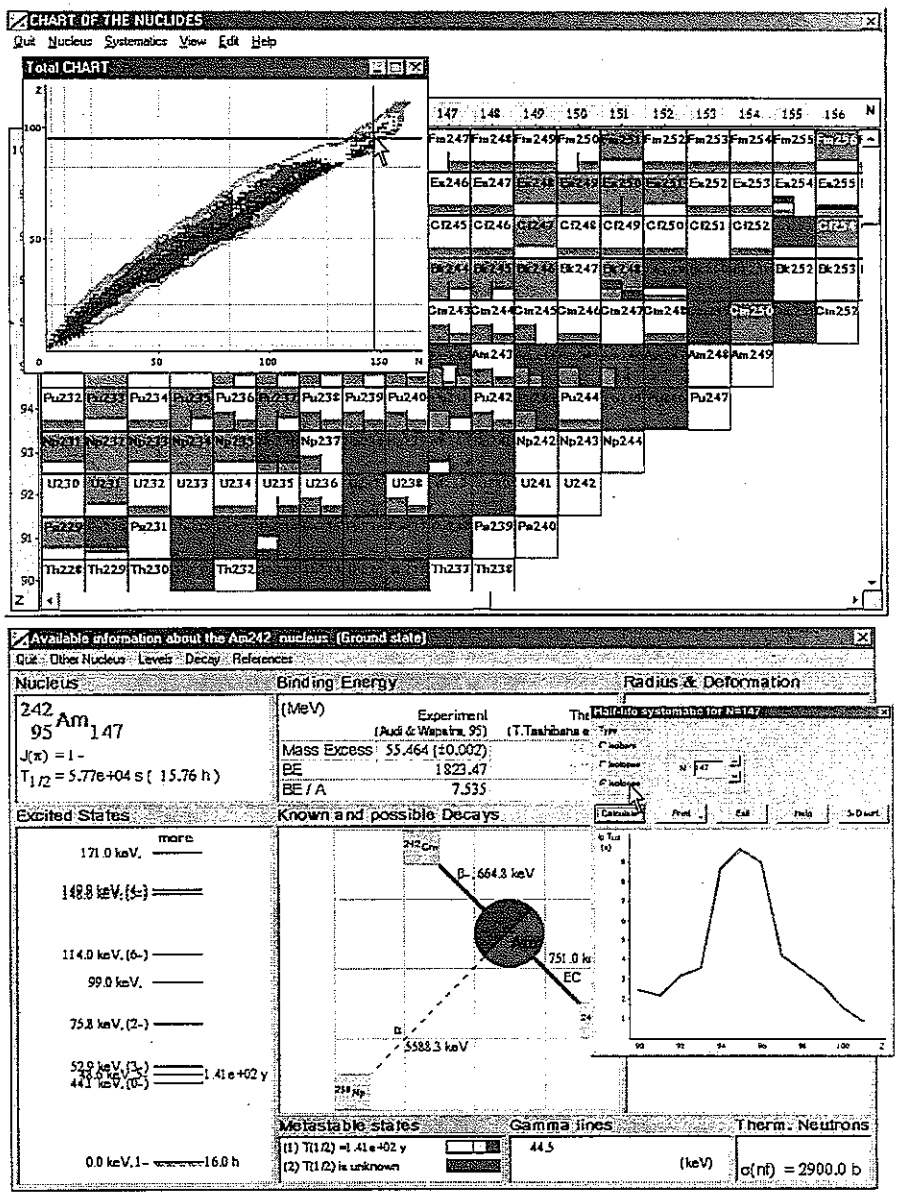

Fig. 6 Nuclear Map and experimental properties of a chosen nucleus

Nuclear database of the NRV consists of three correlated DBF tables containing such properties of atomic nuclei as mass excess and its error, spin, parity, half-life and modes of decay of the ground and metastable states, electromagnetic properties, excited states (energy, spin, parity, half-life), cross section for thermal neutron, γ-lines, and α-decay energies. The structure of these tables allows one to edit them separately and, in particular, add some new characteristics of nuclei. All the data are prepared in the numerical form and can be easily treated inside the codes of the NRV.

There are three main differences between our database of experimental nuclear properties and other well-known nuclear databases [1-8]. (i) All the properties of a given nucleus are shown in one window. (ii) These properties are presented in a visualized graphical form. (iii) A user can easily process these data obtaining additional information (Q-values, decay chains, systematic on any quantity over a group of nuclei) and presenting results in the form he wants.

In Fig.6 the Nuclear Map and the window of the chosen nucleus (here ^{242}Am) are shown together with the dependence of the half-life on the atomic number for all known isotones with N=147 (as an example of one of numerous systematics which can be easily obtained by a simple click of a mouse). Unfortunately, these gray-scaled figures (and all others in the paper) are not so very well seen and easily-read as the corresponding multi-colored versions on a computer screen. Two other systematics (dependence of the energy of the first 2^+ state and of α-particle separation energy on the atomic number of dysprosium isotopes) are shown in Fig.7.

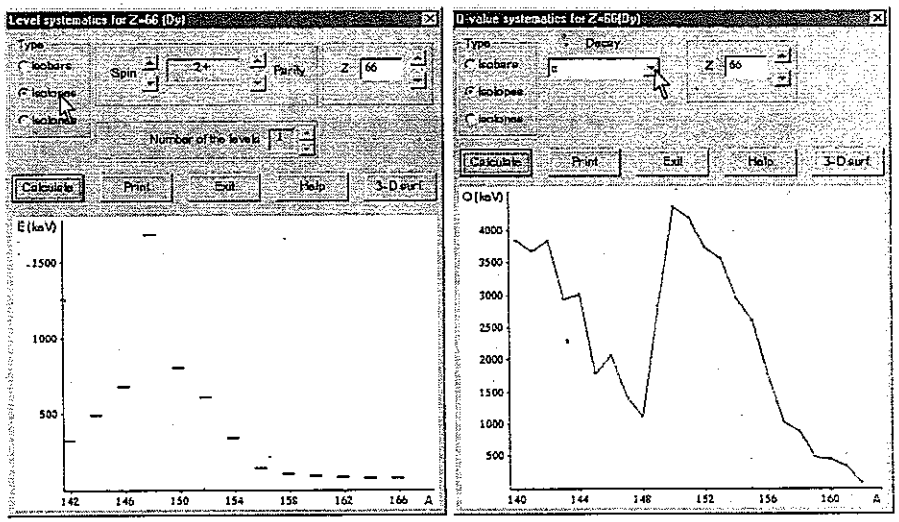

Fig. 7 Two examples of numerous systematics which can be obtained within the NRV. Position of the first 2+ excited states (left) and separation energies of α-particles (right) plotted for different dysprosium isotopes. Both systematics obviously point to the effect of neutron shell with N=82.

4 Elastic scattering

Elastic scattering is essential and sometimes the most important feature of nuclear collisions. On the one hand, from the analysis of elastic scattering data we obtain directly the parameters of the interaction of the colliding particles, i.e., the most fundamental nuclear properties. On the other hand, the dynamics of any nuclear reactions is determined to a considerable extent by "elastic" motion of the colliding particles in the entrance channel and of the formed fragments in the exit one. It means that analysis of any nuclear process should begin from a careful study of elastic scattering of the nuclear particles involved in the process. Here we describe the models of elastic scattering included in the NRV. The other reaction models will be described in our forthcoming publications.

4.1 Classical model of elastic scattering

In spite of essentially quantum properties of nuclear dynamics, many processes can be understood much better and quite clear just within a classical model. If the de Broglie wavelength of the colliding particle relative motion is sufficiently small, then the properties of the corresponding wave function (both the amplitude and the phase shift) are defined mainly by a set of the classical trajectories. Applicability of the classical model (in a sense of fulfillment of the inequality $kR \gg 1$, where k is the wavenumber and R is the characteristic length of the interaction of the colliding particles) is justified at energies $E_{p,n} > 80$ MeV for nucleon-nucleus collisions, at $E_\alpha > 20$ MeV for α-particles, and at all energies for heavy ion collisions.

Within the NRV, description of the Classical Model (as well as the other models) is made by a standard hypertext Windows HELP file with all used formulas, explanatory figures and references. So a user (even inexperienced) in any step of the calculation can easily obtain all needed information to apply the model quite competently.

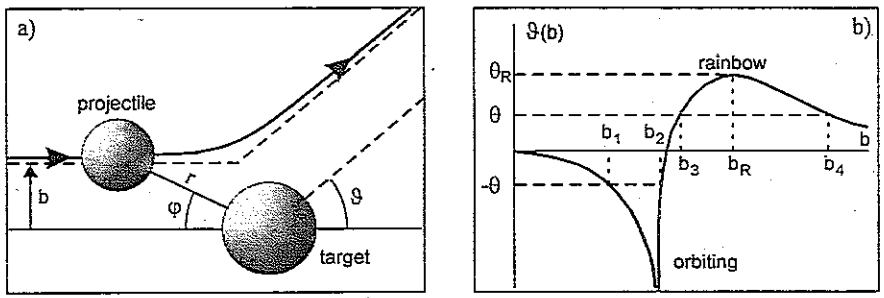

Fig. 8 Classical trajectory, turning angle and deflection angle (a). Deflection function showing the rainbow scattering and orbiting (b).

In the simplified classical model of elastic scattering the projectile and the target are treated as massive points (without any internal structure) interacting by a central potential force deduced from the potential energy $V(r)$ which is a superposition of the Coulomb and the short-range nuclear interactions: $V(r)=V_C(r)+V_N(r)$. In the center-of-mass system the turning angle $\varphi(b,r)$ is defined by the formula $\varphi(b,r) = \int_r^\infty \frac{b}{r^2} \frac{dr}{\sqrt{1-V(r)/E-b^2/r^2}}$ and the total

deflection angle is $\vartheta(b) = \pi - \varphi(b, r_0)$, where b is the impact parameter, r is the relative distance between nuclei, and r_0 is the distance of the closest approach (turning point):

$$1 - V(r)/E - b^2/r^2\big|_{r=r_0} = 0. \qquad (4.1)$$

The Coulomb interaction of two uniformly charged spheres is $V_C = Z_P Z_T e^2 \cdot \frac{1}{r}$ at $r > R_C$ and $V_C = Z_P Z_T e^2 \cdot \frac{1}{2R_C}(3 - \frac{r^2}{R_C^2})$ at $r < R_C$, where $R_C = r_o^c \cdot (A_P^{1/3} + A_T^{1/3})$. Nuclear interaction can be chosen as one of the following potentials: Woods-Saxon volume - $V_N(r) = V_0 \frac{1}{1 + \exp[(r - R_V)/a]}$, Woods-Saxon surface - $V_N(r) = V_0 \frac{\exp[(r - R_V)/a]}{\{1 + \exp[(r - R_V)/a]\}^2}$, with $R_V = r_o^V \cdot (A_P^{1/3} + A_T^{1/3})$, proximity potential [10] - $V_N(r) = 4\pi\gamma \cdot \bar{R} \cdot b \cdot \Phi(\xi)$, with $\gamma = 0.951 \cdot [1 - 1.7826\left(\frac{N-Z}{A}\right)^2] \cdot MeV \cdot fm^{-2}$, $\bar{R} = \frac{C_P C_T}{C_P + C_T}$, $C_i = R_i[1 - \left(\frac{b}{R_i}\right)^2]$, $\xi = \frac{s}{b}$, $s = r - (C_P + C_T)$, and

$$\Phi(\xi) = \begin{cases} -1.7817 + 0.9270\xi + 0.14300\xi^2 - 0.09000\xi^3, & \xi < 0 \\ -1.7817 + 0.9270\xi + 0.01696\xi^2 - 0.05148\xi^3, & 0 < \xi < 1.9475 \\ -4.41 \cdot \exp(-\frac{\xi}{0.7176}), & \xi > 1.9475 \end{cases}$$

or symmetric single-folding potential by Gross and Kalinowski [11] - $V_{GK}(r, R_1, R_2) = \frac{1}{2}\left(\int V_1(r - r', R_1)\rho_2(r', R_2)d^3r' + \int V_2(r - r', R_2)\rho_1(r', R_1)d^3r'\right)$, which can be finally written in a parametric form.

The elastic scattering cross section in the classical model is given as [12]

$$\frac{d\sigma}{d\Omega}(\theta) = \sum_i \frac{b_i(\theta)}{\sin\theta} \cdot \left|\frac{d\vartheta(b)}{db}\right|^{-1}_{b_i(\theta)} \cdot [1 - P_{abs}(b_i)], \qquad (4.2)$$

where b_i is the impact parameter corresponding to the detected angle θ, i.e., $\vartheta(b_i) = \pm\theta$ (see Fig. 8b). The contribution of each trajectory is reduced in accordance with the survival probability by the factor of $1 - P_{abs}(b) = \exp[-\int_{traj(b)} ds/\lambda_{free}(r)]$ taking into account a loss of the incoming flux due to coupling with inelastic channels, here $\lambda_{free} = -\frac{\hbar v}{2W(r)}$ is the mean free path and $W(r) < 0$ is the absorptive potential (imaginary part of the optical model potential). If there is a rainbow in the deflection function ($d\vartheta/db\big|_{b=b_R} = 0$), then its contribution into the cross section is estimated in a semiclassical way [13]:

$$\frac{d\sigma}{d\Omega}(\theta \approx \theta_R) = \frac{2\pi b_R}{k \sin\theta} \cdot |C|^{-2/3} \cdot Ai^2(z) \cdot [1 - P_{abs}(b_R)], \qquad (4.3)$$

where Ai is the Airy function, $C = \frac{1}{2k^2}\frac{d^2\vartheta}{db^2}\big|_{b=b_R}$, and $z = \pm|C|^{-1/3}(\theta - \theta_R)$.

The Classical Model code of the elastic scattering allows a user to obtain and to handle in separate windows the interaction potential, the field of the classical trajectories, deflection function, survival probability, dependence of the turning point on the impact parameter, and the differential cross section, which can be presented in the absolute scale or in the form of the ratio to the Rutherford cross section, in the laboratory or center-of-mass systems. It can be compared with experimental data, and the contributions of different branches of the deflection function and of the rainbow scattering can be easily found and shown, Fig. 9. Only a comparison between the cross section calculated within a quantum model (see below) with the classical cross section, alongside with analysis of the classical deflection function, can provide deep understanding of the properties of investigated angular distribution and dynamics of the elastic scattering.

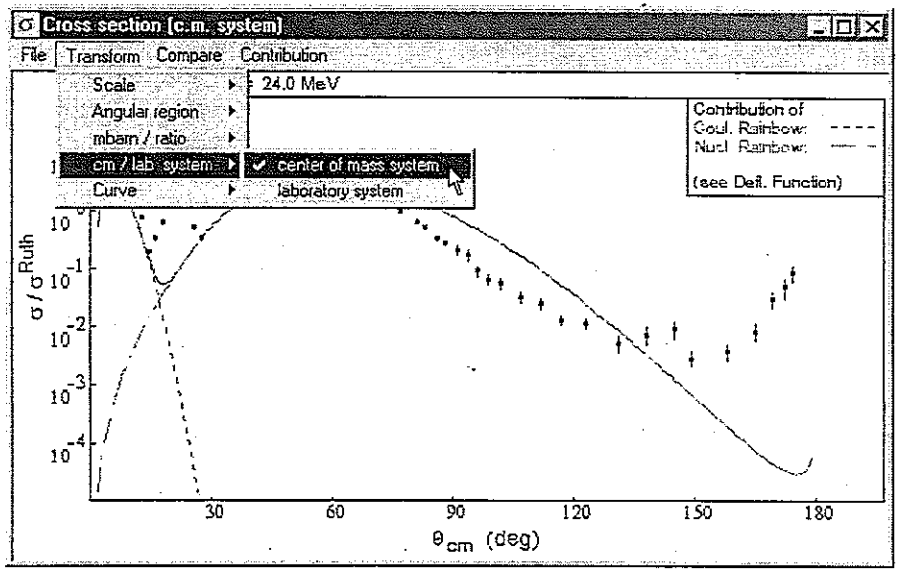

Fig. 9 Cross section window in the Classical Model code of the NRV.

4.2 Semiclassical model of elastic scattering

Semiclassical approximation is very often used in description of the elastic scattering of a nuclear particle. There are two reasons for that. First, within the semiclassical approximation the main quantum effects (interference and barrier penetrability) are taken into account and a calculated result is usually close to an exact one. Secondly, more obvious (trajectory) explanations of the obtained results can be achieved comparing with direct quantum calculations.

The elastic scattering cross section can be written as the sum of two scattering

amplitudes coming from the long-range Coulomb interaction (calculated analytically)

$$f_C(\theta) = -\frac{\eta}{2k\sin^2\theta/2}\exp\left[2i(\sigma_0 - \eta\ln\sin\theta/2)\right], \qquad (4.4)$$

and from the short-range nuclear potential

$$f_N(\theta) = \sum_{l=0}^{\infty}(2l+1)i^{2l}e^{i\sigma_l}\frac{S_l-1}{2ik}P_l(\cos\theta), \qquad (4.5)$$

$$\frac{d\sigma}{d\Omega}(\theta) = \left|f_C(\theta) + f_N(\theta)\right|^2. \qquad (4.6)$$

Here $\sigma_l = \arg\Gamma(l+1+i\eta)$ are the Coulomb phase shifts, $\eta = k(Z_1Z_2e^2)/2E$ is the Sommerfeld parameter, $S_l = \exp(\delta_l)$ are the partial matrix elements, and δ_l are the partial nuclear phase shifts which can be calculated numerically by solving the radial Schrödinger equations (see below the Optical Model).

In the semiclassical approximation the total (Coulomb + nuclear) partial phase shift can be found as follows

$$\delta_l + \sigma_l = kb\frac{\pi}{2} - kr_0(b) + \eta\ln 2kr + \int_{r_0(b)}^{\infty}[k(b,r) - k + \frac{\eta}{r}]dr, \qquad (4.7)$$

where $k(b,r) = k\sqrt{1 - V(r)/E - b^2/r^2}$ is the local wavenumber, $r_0(b)$ is the turning point of the trajectory with the impact parameter $b = (l+1/2)/k$. In the general case there are several complex solutions of Eq. (4.1) for the turning points. Imaginary part of $r_0(b)$ arises due to a possibility of the above-barrier reflection of an incoming wave and due to imaginary part of the OM potential. As a result, we have to use not a very simple complex trajectory approach for adequate description of the elastic scattering within semiclassical approximation [14]. However, in many cases for the Woods-Saxon type OM potentials the complex turning points can be given in a parametric form [15] and the cross section is easily calculated.

In many cases the radial partial wave functions or the 3-dimensional distorted wave in the elastic channel are also needed. They can be obtained in an exact form just from the Schrödinger equation or calculated in semiclassical approximation [16]. In particular, for the Coulomb scattering (sub-barrier energies) all the quantities can be found in an analytical form [16]: the Coulomb phase shifts $\sigma_l^{SC} = \eta\ln\sqrt{(kb)^2+\eta^2} + kb\cdot arctg(\eta/kb) - \eta$, the turning angle $\varphi_C(b,r) = arctg\frac{kb/r + \eta/b}{k(b,r)} - arctg\frac{\eta}{kb}$, the turning point $r_0^C = \frac{\eta}{k} + \sqrt{(\eta/k)^2 + b^2}$, the Coulomb partial waves (regular solution)

$$F_l(r) = \begin{cases}\sqrt{\frac{k}{k(b,r)}}\sin[\eta + k(b,r)r - \eta\cdot\ln(k(b,r)r + kr - \eta) + kb\cdot\varphi_C(b,r) + \sigma_l^{SC} - l\pi/2], & r > r_0\\ \sqrt{\pi k}\cdot\xi^{-1/3}\cdot Ai[\xi^{-2/3}(r - r_0)], & r \le r_0\end{cases}$$

with $\xi^2 = k^2(r_0^2 + b^2)/r^3$. Finally, the Coulomb distorted wave in the 3-dimensional space divided by the Coulomb caustic surface $\vartheta_C(r) = \arccos(1 - 4\eta/kr)$ onto the classically forbidden region ($\theta < \vartheta_C(r)$) and the region where two trajectories with impact parameters $b_{1,2}(r,\theta) = \frac{r\cdot\sin\theta}{2}\{1 \pm \sqrt{1 - \frac{4\eta}{kr}\frac{1}{(1-\cos\theta)}}\}$ pass through each point (r,θ), can be written as

$$\Psi_k^{C(+)}(r,\theta) = \begin{cases} A_1\cdot e^{iS_1(r,\theta)} + A_2\cdot e^{iS_2(r,\theta)}, & \theta > \vartheta_C(r)\\ \sqrt{\pi}(2\eta)^{1/6}Ai\left[\frac{k(\varsigma_C - \varsigma)}{2(2\eta)^{1/3}}\right]\cdot\exp[i(kr - 3\eta + \eta\ln\eta + \frac{k}{2}((\varsigma_C - \varsigma) - \frac{\pi}{4})], & \theta \le \vartheta_C(r)\end{cases}$$

where $A_1 = \frac{\beta}{2}(1-\alpha)^{-1/4}$, $S_1 = k(\varsigma+\tau)/2 - k\varsigma + \eta\ln k\varsigma + 2\eta\ln(\beta/2) + \eta\alpha/\beta^2$,

$A_2 = \frac{\eta}{k\varsigma(1-\alpha)^{1/4}}(1 + \frac{\alpha}{\beta^2})$, $S_2 = k(\varsigma+\tau)/2 - \eta\ln k\varsigma - 2\eta[1 + \alpha/2\beta^2 - \ln(1+\alpha/\beta^2)] - \pi/2$,

$\varsigma = r\cdot(1-\cos\theta)$, $\tau = r\cdot(1+\cos\theta)$, $\varsigma_C = \varsigma(r,\vartheta_C)$, $\alpha = 4\eta/k\varsigma$, $\beta = 1 + \sqrt{1-\alpha}$.

4.3 Optical model of elastic scattering

In a quantum mechanical Optical Model of elastic scattering (OM) the relative motion of the projectile and target is described by an effective one-body Scrödinger equation [17]

$$\left[-\frac{\hbar^2}{2\mu}\Delta + V_{OM}\right]\cdot\Psi_{\vec{k}}^{(+)}(r,\theta) = E\Psi_{\vec{k}}^{(+)}(r,\theta) \qquad (4.8)$$

where $E = \hbar^2k^2/2\mu$ is the relative motion energy, μ is the reduced mass, and V_{OM} is the effective non-hermitian operator named optical potential (OP). Here it is assumed that an influence of all the reaction channels on the elastic one can be simulated by an appropriate choice of the OP. In practice the phenomenological OP with a simple radial dependence is usually used

$$V_{OM}(r) = V_C(r) + V_N(r) + iW(r) + [V_{so}(r) + iW_{so}(r)]\cdot(\vec{l}\cdot\vec{s}). \qquad (4.9)$$

Here the Coulomb and nuclear interactions V_C+V_N are the same as above (see Classical Model), the imaginary part of OMP is chosen in the volume or surface Woods-Saxon forms, or as their superposition. The spin-orbital interaction V_{so}+iW_{so} can be included when the projectile has a non-zero spin.

The relative motion wave function has the outgoing boundary condition at infinity

$$\Psi_{\vec{k}}^{(+)}(r,\theta) \approx e^{ikr\cos\theta} + f(\theta)\frac{e^{ikr}}{r}, \qquad (4.10)$$

where $f(\theta)$ is the scattering amplitude (this formula should be slightly modified for the scattering of charged particles due to a long-range Coulomb interaction distorting the plane wave and the outgoing spherical wave at large distances). To find the scattering amplitude, the total wave function has to be decomposed into the partial waves

$$\Psi_{\vec{k}}^{(+)}(r,\theta) = \sum_{l=0}^{\infty}(2l+1)i^l\psi_l(r)P_l(\cos\theta), \qquad (4.11)$$

and then one-dimensional radial Scrödinger equations are to be integrated numerically from $r=0$ up to some large distance $r=R_{max}$, where $V_N(r)$ and $W(r)$ can be neglected and only the Coulomb interaction remains. At this large distance the numerical solution is smoothly joined with a known asymptotic behavior of the partial wave

$$\psi_l(r) \approx e^{i\sigma_l}\frac{1}{2}\left[(F_l + iG_l) + S_l(F_l - iG_l)\right], \qquad (4.12)$$

where F_l and G_l are the regular and irregular Coulomb partial wave functions. Having found in this way the partial S-matrix elements, the nuclear scattering amplitude can be then calculated with (4.5) and the differential cross section of elastic scattering with (4.6).

For a deeper insight into the mechanism of the elastic scattering (nature of the interference pattern, rainbow effects, etc.) the classical and semiclassical models described above can be used simultaneously alongside with the OM calculations. However, within the OM, the so called "near-far" decomposition of the scattering amplitude can be also made, which gives in many cases much better understanding of some specific features of the angular distribution [18,19]. Such decomposition is an identical transformation of (4.5) based on the representation of the Legendre polynomials in the form

$$P_l(\cos\theta r) = \tilde{Q}_l^{(+)}(\theta r) + \tilde{Q}_l^{(-)}(\theta r) \qquad (4.13)$$

with the asymptotic $\tilde{Q}_l^{(\pm)}(\theta r) \approx [\pi(2l+1)\sin\theta]^{-1/2}\exp\{i[\pm(l+1/2)\theta \mp \pi/4]\}$ at $l >> 1/\sin\theta$. Placing (4.13) into (4.5) one obtains the "near-far" decomposition, which shows, in the short-wave limit ($L_{max} \cong kR_{max} >> 1$), the contributions to the amplitude coming from the scattering to positive angles ("near", $2d\delta_l/dl = \vartheta(b) = +\theta$) and to negative angles ("far", $2d\delta_l/dl = \vartheta(b) = -\theta$).

For a given set of the OM parameters the Optical Model code of the NRV allows one to calculate and present in graphical and tabular forms all the quantities mentioned above: the partial waves $\psi_l(r)$, the partial matrix elements S_l, the total wave function in the 3-dimensional space $\Psi_{\vec{k}}^{(+)}(r,\theta)$, and the differential cross section $d\sigma/d\Omega$. (Fig.10). An automatic search of the OMP parameters can be fulfilled with a fit of the calculated elastic scattering angular distribution to the available experimental data. Many additional possibilities are also included to the Optical Model code which allows one to analyze an investigated process in detail.

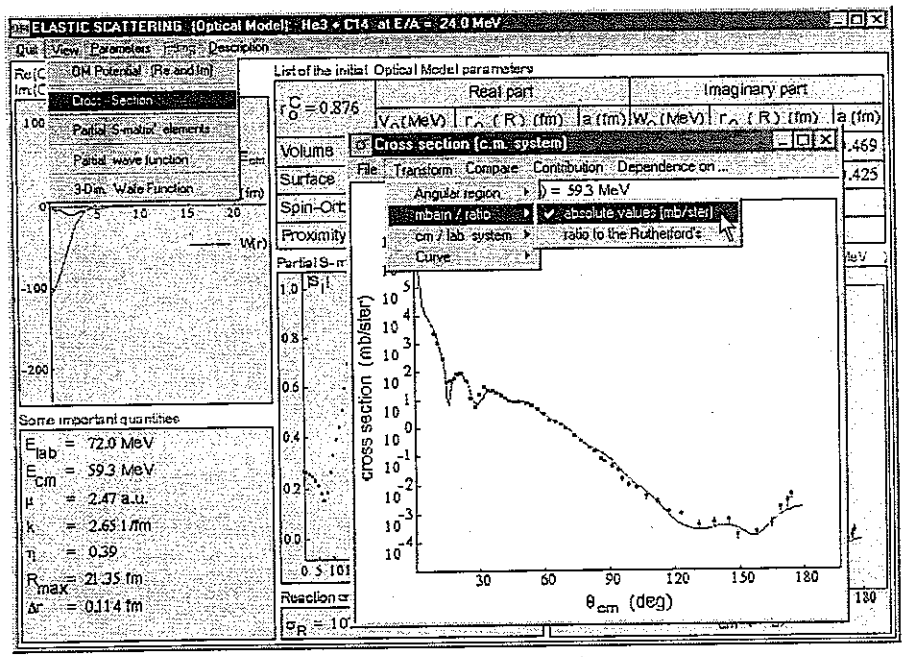

Fig. 10 Main screen of the Optical Model code and one of its windows.

5 3-dimensional graphics of the NRV

Special attention in the NRV is paid to a visualized presentation of all the quantities. In particular, internal graphic editor allows one to draw and handle 3-dimensional and topographical plots directly during the calculations, see Fig. 11 as an example. A user can choose an appropriate type of the surface (simple grid, multi-colored, lighted, 3-dimensional bars), rotate the surface, print it, or save the table for other applications. All the possibilities of the NRV graphical editor will be also described in our forthcoming papers.

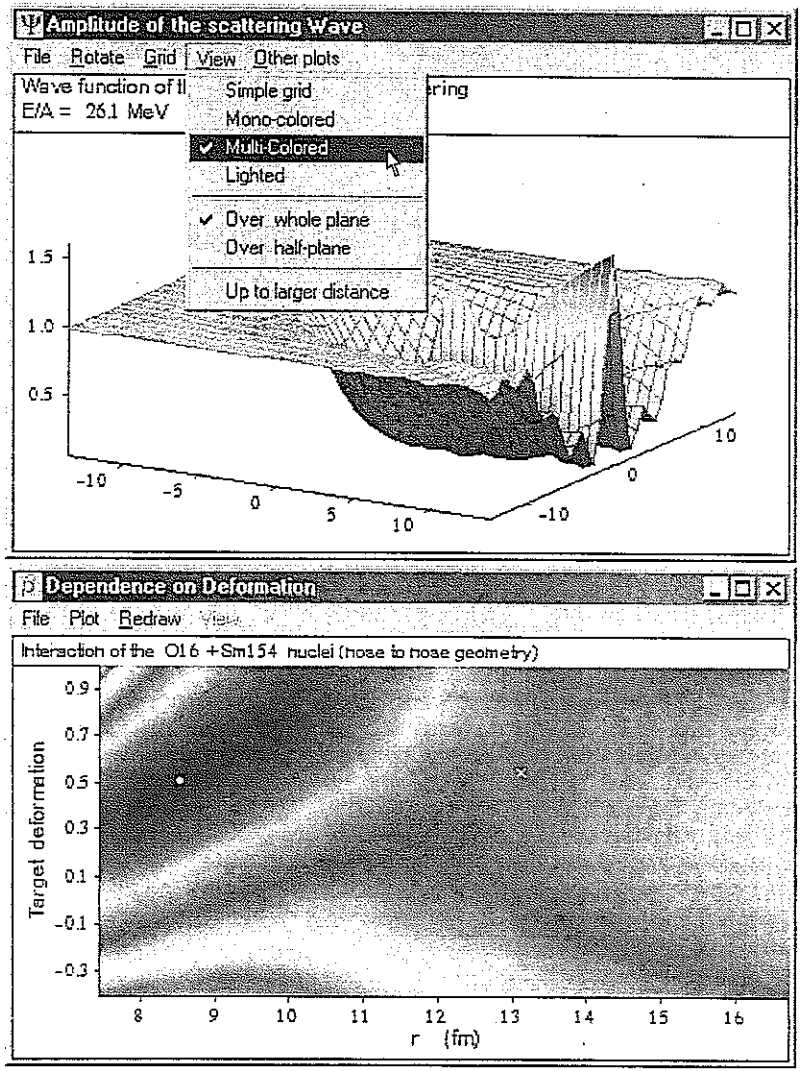

Fig. 11 Amplitude of the ^{8}He+^{4}He wave function and potential energy of ^{16}O+^{154}Sm.

References

[1] Atomic Mass Data Center (Orsay), http://csnwww.in2p3.fr/amdc/amdc_en.html, G.Audi, A.H.Wapstra, Nucl.Phys., **A595** (1995), 409; ibid. **A624** (1997), 1.

[2] National Nuclear Data Center, Brookhaven National Laboratory, http://www.nndc.bnl.gov/, Web coordinator – T.W.Burrows.

[3] Nuclear Data Services, Nuclear Energy Agency, France, http://www.nea.fr/html/dbdata/.

[4] IAEA's Nuclear Data Centre, http://iaeand.iaea.or.at/.

[5] Center for Photonuclear Experimental Data, Moscow State University, http://depni.npi.msu.su/cdfe, V.V.Varlamov.

[6] Nuclear Data Center, Japan Atomic Energy Research Institute, http://wwwndc.tokai.jaeri.go.jp/.

[7] Lund Nuclear Data WWW Service, http://nucleardata.nuclear.lu.se/nucleardata/.

[8] Isotopes Project, LBNL, http://isotopes.lbl.gov/isotopes/ip.html.

[9] S.Y.F.Chu, H.Nordberg, R.B.Firestone, L.P.Ekström, Isotope Explorer, http://ie.lbl.gov/isoexpl/isoexpl.htm.

[10] J.Blocki, J.Randrup, W.J.Swiatecki, C.F.Tsang, Ann. Phys.(N.Y.), **105** (1977), 427.

[11] D.H.E.Gross, H.Kalinowski, Phys. Reports, **45C** (1978), 175.

[12] R.Newton, Scattering Theory of Waves and Particles, McGraw-Hill Book Company, 1966, Ch.5 and Ch.18.

[13] K.W.Ford, J.A.Wheeler, Ann. Phys.(N.Y.), 7 (1959), 259.

[14] E.Vigezzi, A.Winther, Ann. Phys.(N.Y.), 192 (1989), 432.

[15] D.Semkin, V.Zagrebaev, Izv. AN, ser.fiz., **58** (1994), 109 (in Russian).

[16] V.I. Zagrebaev, Ann.Phys.(N.Y.), **197** (1990) 33.

[17] P. Hodgson, The Optical Model of Elastic Scattering, Oxford Univ. Press (Clarendon) London, 1963.

[18] R.S. Fuller, Phys.Rev., **C12** (1975) 1561.

[19] M.S. Hussein, K.W. McVoy, Progr.Part.Nucl.Phys., **12** (1984) 103.

Received by Publishing Department
on May 20, 1999.